J Solid State Electrochem (2010) 14:543–548
DOI 10.1007/s10008-008-0659-3

ORIGINAL PAPER

A structural influence on the electrical double-layer characteristics of Al_4C_3-derived carbon

Marko Lätt · Maike Käärik · Liina Permann · Helle Kuura · Mati Arulepp · Jaan Leis

Received: 2 June 2008 / Revised: 15 August 2008 / Accepted: 19 August 2008 / Published online: 10 September 2008

Abstract Several carbon materials were produced by reacting aluminum carbide with chlorine gas at different temperatures (400–900 °C). Chlorination temperature and porosity values showed the inversely related trends whereby the graphitization degree rises with the chlorination temperature. Electrochemical measurements performed in three-electrode test cells with 1.0-M Et_3MeNBF_4 electrolyte revealed that the changes in porosity parameters and the degree of graphitization are in good correlation with specific capacitance values. Capacitance depends on the structure of carbon and varies in studied chlorination range from 109 to 60 F g^{-1} and from 114 to 64 F g^{-1} for the negatively and positively charged electrode materials, respectively. An exceptionally low capacitance was observed for the material produced at 700 °C that was explained by the multiwall carbon nanobarrels and the highly ordered curved graphitic flakes, which have low specific surface and possess the relatively low specific surface-related capacitance.

Keywords Carbide-derived carbon · Electrical double layer · Graphitization · Supercapacitor · Adsorption

Contribution to the Fifth Baltic Conference on Electrochemistry

M. Lätt · M. Käärik · L. Permann · H. Kuura · M. Arulepp · J. Leis
Tartu Technologies Ltd.,
185 Riia Street,
Tartu, Estonia

M. Lätt (✉) · M. Käärik · H. Kuura · J. Leis
Institute of Chemistry, University of Tartu,
2 Jakobi Street,
Tartu, Estonia
e-mail: markx@ut.ee

Introduction

A progress in the field of high-power electrical double-layer (DL) capacitors or so-called supercapacitors requires better electrode materials than the common activated carbons [1]. The alternative carbon, the carbide-derived carbon (CDC), was suggested as promising active material for the electrodes [2]. Still lately, it was generally accepted that the DL capacitance is proportional to the specific surface area [3]. However, it is now clear that not only surface area but also the pore size plays an important role in the double-layer capacitance of carbon [4]. Very recent studies, more so, have indicated that the pores, which diameters are comparable to the dimensions of the adsorbing ions, led to the unexpected increase in the DL capacitance [5]. The authors partly explained it by the contraction of ions in the high dielectric environment.

It is already demonstrated and proven in practice that the highly nanoporous CDC materials, mainly derived from titanium carbide but also from silicon carbide, possess the exceptionally high volumetric capacitance [6, 7]. Quite usually, the term CDC is used as a general reference to all carbide-derived carbons [8, 9]; however, the properties and microstructure of particular carbons may be very different. Commonly, the CDCs are made by etching the carbide with the chlorine at high temperature, which may vary from 200 to 1,200 °C. Of course, it is possible to perform the reaction at even higher temperatures but above ~1,300 °C CDCs undergo the bulk graphitization and therefore have less interest. General reaction scheme describing the CDC formation is as follows:

$$MC_x + y/2Cl_2 \rightarrow xC + MCl_y$$

where M is the carbide forming metal or metalloid and x and y are the stoichiometric constants. Several studies

performed with different carbides have clearly confirmed the significance of the carbonization conditions, such as temperature, mass transfer of reagents, crystal structure of carbide, etc., to the resulting CDC material [5, 10, 11]. What is important, all these factors have different effects when different carbide is carbonized.

Considering the availability of so many variables, which influence the CDC, and the numerous modifications in the microstructure and adsorption behavior consequently possible to achieve, it is evident that only a small part of CDC materials is investigated for different applications. This study was made to learn the electrochemical performance, particularly double-layer characteristics, of Al_4C_3-derived carbons, which are known to have a large variability in graphitization and porosity as the effect of carbonization temperature. Therefore, it was also hoped that the results enable to give some general dependencies of EDL performance from the different structural characteristics, which can at least partly be generalized to all CDC materials.

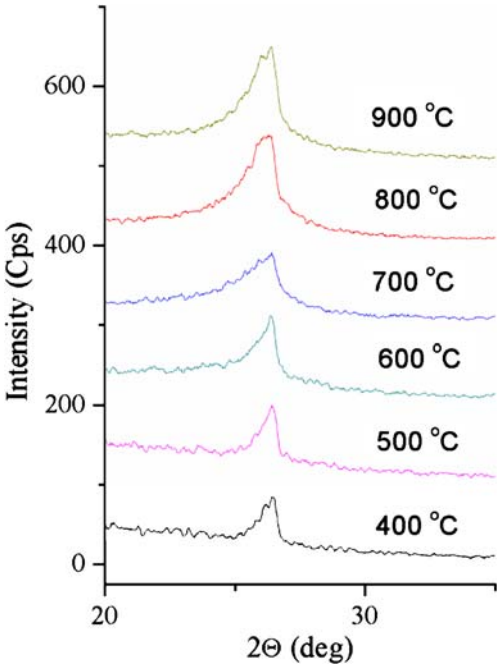

Fig. 1 Bragg 002 diffraction pattern for Al_4C_3-derived carbons made at temperatures noted in figure

Experimental

Several carbon materials (1–6) were produced by etching aluminum carbide (AEE, 1–5 μm) with chlorine gas (AGA, 99.98%) in a stationary bed reactor at different temperatures (400–900 °C) During heating and cooling, the reactor core was flushed with argon gas to prevent any contaminants from entering the reaction zone. During etching, chlorine gas was administered at a rate of 1.5 l min^{-1}. The resulting aluminum chloride was carried out of the reactor by excess chlorine and neutralized with sodium hydroxide solution. The chlorination reaction can be described as:

$$Al_4C_3 + 6Cl_2 \rightarrow 3C + 4AlCl_3$$

Carbon materials obtained from the chlorination reaction were posttreated in a separate stationary bed reactor with hydrogen gas (AGA, 99.9995%) at 800 °C to dechlorinate them and remove any oxygen-containing functional groups from the active surface of carbon. To determine the completion of the dechlorination reaction, the pH of the gas exiting the reactor was monitored. As it approached the neutral region of the pH scale, the reaction was deemed complete.

Benzene adsorption (W_s) was measured by using computer-controlled (HS-202) weighing of carbon samples in benzene vapor. Measurements were performed at room temperature and atmospheric pressure.

The low-temperature nitrogen adsorption experiments were performed using Gemini Sorptometer 2375 supported by Stardriver software. Carbon samples were heated in vacuum at 300 °C and saturated with argon gas before performing the measurements. Specific surface area, S_{BET}, of the samples was calculated according to BET theory. Distribution of pore sizes and the volume of pores (V_{tot}, V_{micro}) were calculated from adsorption and desorption isotherms by applying BJH theory. The average pore size (APS) was derived from the equation:

$$APS = 2V_{tot}/S_{BET}$$

where V_{tot} is the total pore volume measured at near to nitrogen saturation pressure (P/P_0=0.95).

The wide-angle X-ray powder diffraction measurements were performed using CuKα radiation (λ=1.54 Å). Powder sample with a thickness of 1 mm was placed on a plastic holder and the diffraction spectra were recorded at room temperature and analyzed with EVA 5.0 and Origin computer software.

The electrochemical measurements were performed with the Solartron 1287 potentiostat and FRA analyzer in three-

Table 1 Porosity parameters of Al_4C_3-derived carbons

#	T_{Chlor} [°C]	W_s [cm^3 g^{-1}]	S_{BET} [m^2 g^{-1}]	V_{tot} [cm^3 g^{-1}]	V_{micro} [cm^3 g^{-1}]	APS [nm]
1	400	0.57	1,285	0.64	0.51	1.0
2	500	0.64	1,470	0.74	0.57	1.0
3	600	0.69	1,401	0.78	0.46	1.1
4	700	0.75	1,059	0.82	0.16	1.5
5	800	0.66	1,135	0.93	0.22	1.6
6	900	0.69	1,161	0.93	0.29	1.6

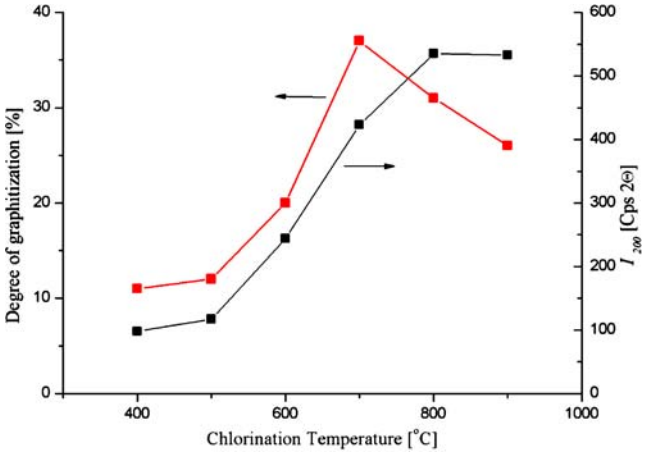

Fig. 2 Influence of the chlorination temperature on the structural order of Al_4C_3-derived carbons

electrode test cells with 1.0-M Et_3MeNBF_4–propylene carbonate electrolyte. During experiments, the electrolyte was degassed with argon. Experiments using constant voltage (CV) and constant current (CC) techniques were carried out. Discharge capacitance for the negatively and positively charged electrode materials was calculated from the CC plots.

Results and discussion

Structural characteristics of Al_4C_3-derived carbons

The low-temperature nitrogen sorption of carbon samples (1–6) synthesized at temperatures between 400 and 900 °C revealed that the average pore size of those samples, represented in Table 1, is strongly influenced by the structural order created during carbonization of the carbide.

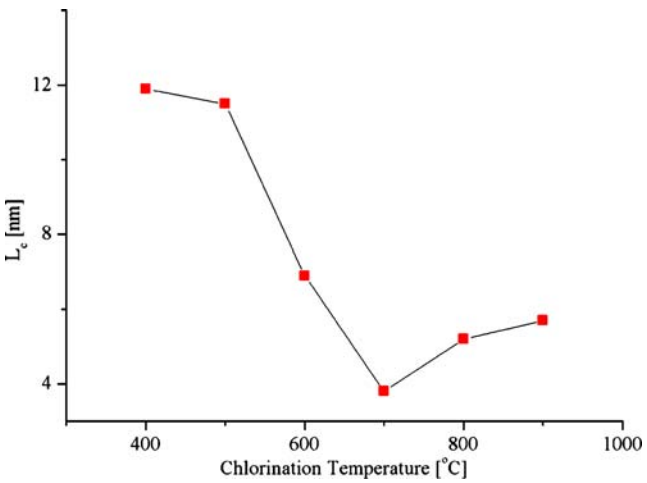

Fig. 3 The thickness of crystallites, L_C, for Al_4C_3-derived carbons made at different temperatures

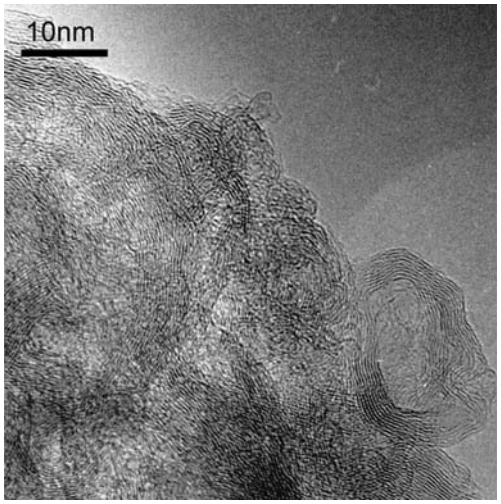

Fig. 4 The HRTEM picture of highly graphitized carbon made from Al_4C_3 at 700°C

An increase in the structural order with increasing the synthesis temperature was monitored by the Bragg 002 signal in X-ray diffraction (XRD) profiles as shown in Fig. 1.

Increasing of the APS with the synthesis temperature is obviously caused by the mesopores and voids formed between structurally ordered (graphitic) fragments. This assumption is in agreement with the reversed trends in the temperature dependence of the volume of micropores (V_{micro}) and the total pore volume (V_{tot}). The analysis of specific surface areas (S_{BET}), which are proportional to the values of V_{micro}, proves that the carbons made at the temperature below 700 °C possess the largest surface and microporosity. Therefore, one may assume that the samples 1–3 also have the best EDL capacitance. However, it is interesting to note that the pore volume according to benzene (W_s) follows better the V_{tot} rather than V_{micro}

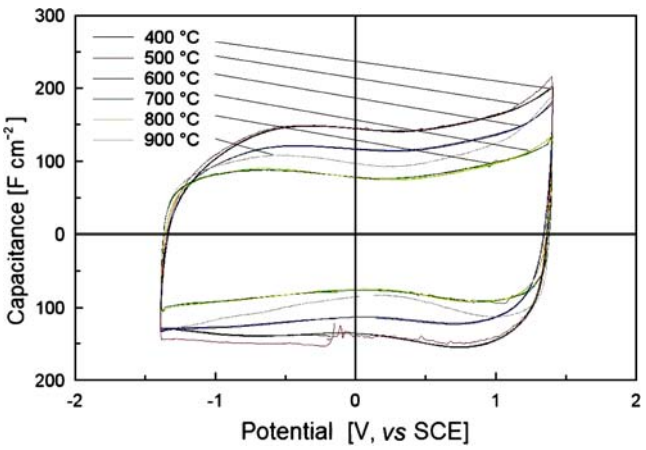

Fig. 5 Capacitance vs. potential for different Al_4C_3-derived carbons in 1.0-M Et_3MeNBF_4 propylene carbonate solution calculated from *j*, *E*-plots at sweep rate v=5 mV s^{-1}

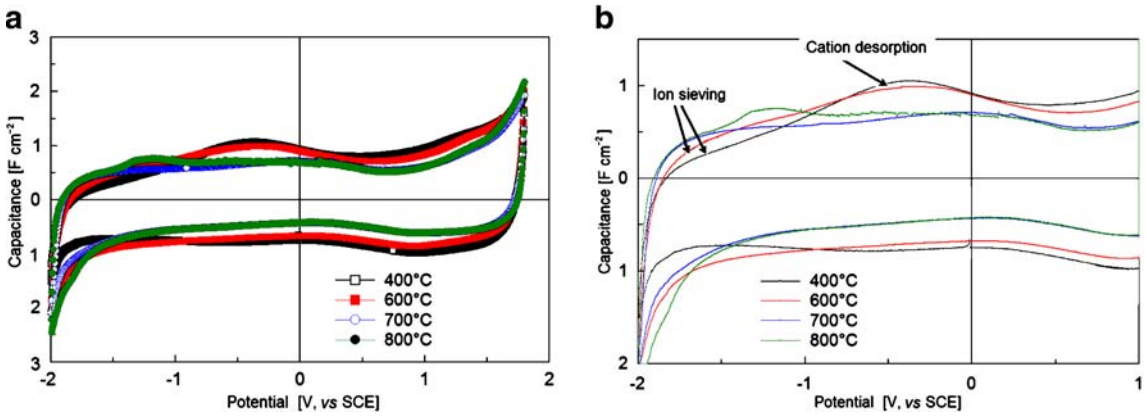

Fig. 6 **a**, **b** Capacitance vs. potential for different Al_4C_3-derived carbons in 1.0-M Et_3MeNBF_4 propylene carbonate solution calculated from CV plots at sweep rate v=2 mV s^{-1}

values, which means that the mesopores still may give a significant contribution into the adsorption of relatively small electrolyte ions from condensed phase, i.e., in double-layer capacitance.

The degree of graphitization, q, i.e., the relative amount of graphene sheets parallelly oriented in the multilayered stacks was estimated from the equation:

$$q = \frac{I_{002}/I_{10}}{14.3}\,100\%$$

where I_{002} and I_{10} are the intensities of corresponding XRD patterns and the empirical constant 14.3 is derived for the completely graphitized pyrolytic carbon without amorphous phase [12]. The dependence of the degree of graphitization on the temperature of carbide chlorination observed and presented in Fig. 2 is in a good agreement with the previous studies about CDC-type materials [10, 13].

The size of crystallite or, in other words, the thickness of graphitic structures in 002 directions was calculated from Scherrer formula:

$$L_C = K\lambda/\beta\cos\Theta,$$

where K is a constant depending on the reflection plane (0.89 for 002 peak, λ is the wavelength of the X-ray (0.154 nm), Θ is the position of the peak and β is the half-height width of the peak in 2Θ (rad) units.

Unexpectedly, the L_C values in Fig. 3 turned out being reversely related to the degree of graphitization. One of the explanations could be that the increase in chlorination temperature increases the average structural order, but the multilayered graphitic structures formed are highly curved and therefore possess a poor crystallinity. Previous structural studies on Al_4C_3-derived carbons have shown that the

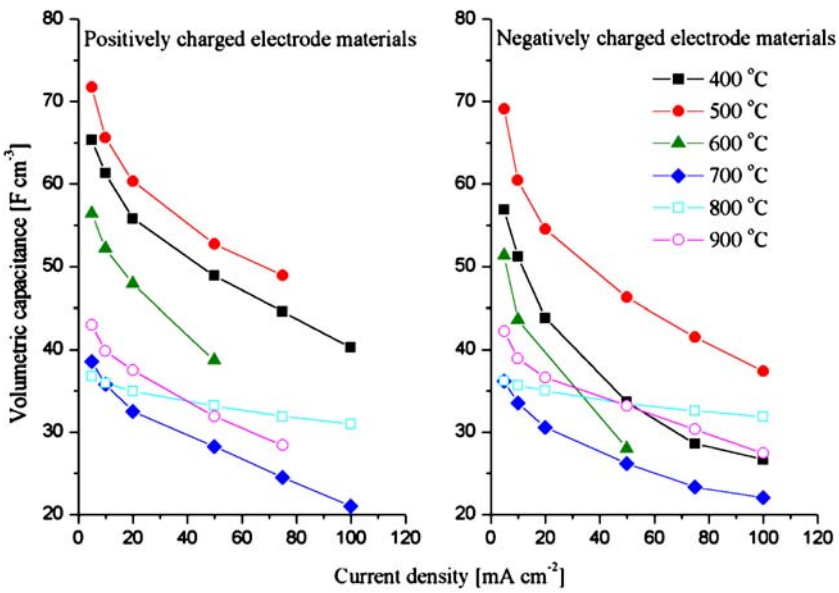

Fig. 7 Volumetric capacitance calculated at different current densities for different Al_4C_3-derived carbons synthesised at temperatures as noted in figure

range of chlorination temperatures of 600–800 °C increases the tendency to form hollow semispherical carbon nanoparticles, so-called nanobarrels [10]. The electron microscopy pictures of the carbons of this study also confirm the curved graphitic ribbons and flakes (see Fig. 4), which partly explains the observed L_C minima at 700 °C in Fig. 3.

Electrochemical evaluation

The polarizable electrodes from Al_4C_3-derived carbon powders were manufactured as follows. The mixture of 94 wt.% nanoporous carbon and 6 wt.% poly(tetrafluoroethylene) binder (Aldrich, 60% suspension in water) was rolled stepwise into the carbon film with a final thickness of 100±5 μm. After drying, the raw electrode sheets were plated from one side with a thin aluminum layer (2±1 μm) using the plasma-activated physical vapor deposition.

Disc-shaped carbon electrodes (0.43 cm^2) were investigated using three-electrode setup. Before experiments, the carbon electrodes were vacuum-dried at 180 °C for 2 h. The standard glass cell with large counter electrode (apparent area of ~30 cm^2) and saturated calomel electrode (SCE) were used.

The cyclic voltammetry j, E curves were measured in 1.0 M Et_3MeNBF_4 propylene carbonate at scan rates of 2–50 mV s^{-1}. The experimental data show that the shape of j, E curves is independent of the sequential number of a cycle n when $n \geq 5$. At small scan rates of 5 mV s^{-1}, j, E curves with the nanoporous carbon electrodes demonstrate a smooth curve in the region of potentials from −1.4 to +1.4 V (vs. SCE), indicating that the carbon electrodes are ideally polarizable in this region (Fig. 5).

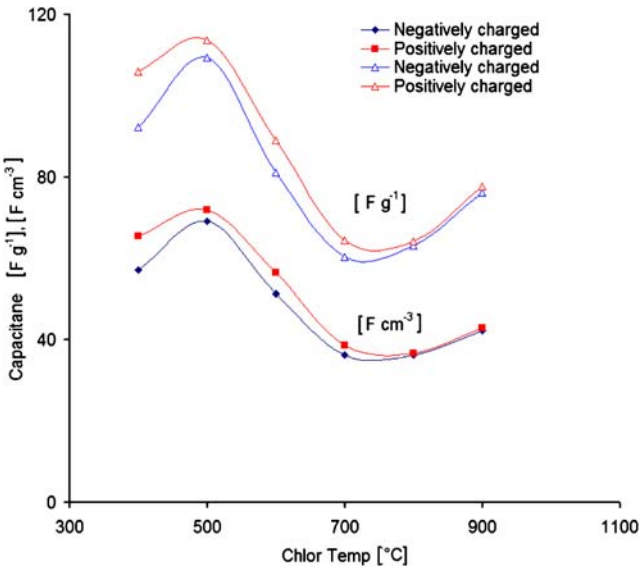

Fig. 8 Specific capacitance [F g^{-1}, F cm^{-3}] for different Al_4C_3-derived carbons in positively and negatively charged electrode potentials calculated at i=5 mA cm^{-2}

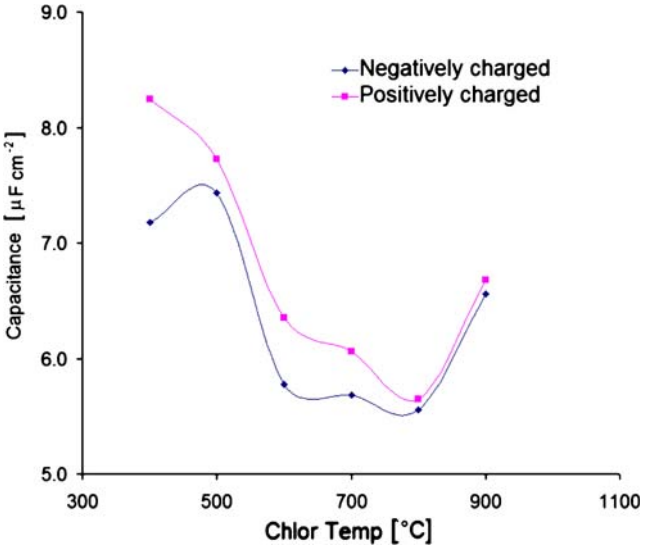

Fig. 9 Specific surface-related capacitance [μF cm^{-2}] for different Al_4C_3-derived carbons at positively and negatively charged electrode potentials calculated at i=5 mA cm^{-2}

Furthermore, it is seen in Fig. 6 that the region of ideal polarizability (ΔE) of the nanoporous carbide-derived carbon electrodes safely exceeds 3.5 V.

At the negatively charged potentials, the so-called ion sieving effect will be observed (Fig. 6b), as in [14–16]. This effect is particularly characteristic for the CDC made at low temperatures (e.g., sample 1). At higher scan rates, $\nu \geq 10$ mV s^{-1}, the j, E curves recorded in propylene carbonate solution become distorted from the mirror-image symmetry. It is caused by the high resistivity of the electrolyte in the porous material. It should be noted that the establishment of the adsorption equilibrium in nanopores is a very slow process.

The capacitance values calculated at CC regimes at current densities of 5–100 mA cm^{-2} are presented in Fig. 7. The capacitance calculated at higher current densities have smaller values as also noted in many papers [7, 17–19]. The

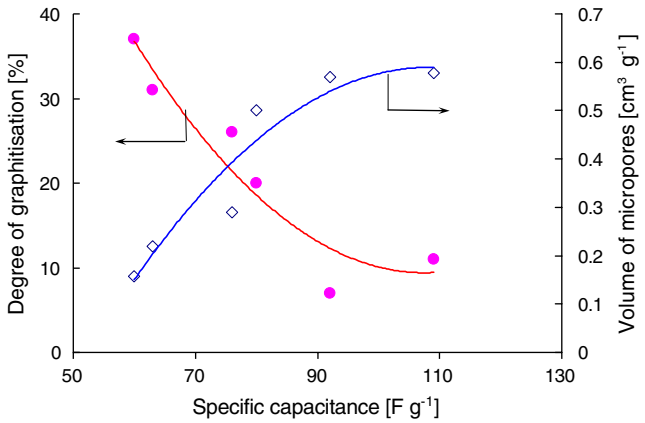

Fig. 10 The influence of structural parameters on the capacitance of Al_4C_3-derived carbon

lowest dependence of d*C*/d*I* was observed for CDC synthesized at 800 °C. The lowest dependence of d*C*/d*I* has the CDC synthesized at 800 °C, which is partly explained by better access to the surface of relatively graphitic carbon with the highest average pore size among the samples studied.

The experiments revealed that changes in porosity parameters and the degree of graphitization are in good correlation with specific capacitance values. Capacitance depends on the structure of carbon and varies in studied chlorination range from 69 to 37 F cm^{-3} and from 72 to 37 F cm^{-3} for the negatively and positively charged electrode materials, respectively, as shown in Fig. 8.

An exceptionally low capacitance was observed for the material produced at 700 °C, which is in good agreement with the above discussed structural characteristics. Particularly in the range of chlorination temperatures 600–800 °C, the highly curved graphite flakes and nanobarrel-like carbon structures are formed. The surface-related specific capacitance of Al_4C_3-derived carbon has different shape for negatively and positively charged electrode potentials (cf. Fig. 9). A clear minimum at positively charged electrode potentials is observed for the sample made at 800 °C. This minimum is due to low specific adsorption of the BF_4^- anions on the curved graphene flake edges. However, the Et_3MeN^+ has bigger cation size and consequently lower accessibility on the CDC surface and therefore the minima for these adsorbed ions are larger [20].

Chlorination temperature and porosity values show inversely related trends (see Fig. 10). Carbon materials produced at lower chlorination temperatures yield higher BET surface areas and exhibit higher specific capacitance. Graphitization, which rises with the chlorination temperature, decreases the specific capacitance of Al_4C_3-derived carbons.

Conclusion

A set of carbon powders was made by chlorinating aluminum carbide at the varied temperatures in the range of 400–900 °C. As expected, the chlorination temperature and porosity values showed inversely related trends. Carbon materials produced at lower chlorination temperatures yield higher BET surface areas and exhibit higher specific capacitance. Graphitization degree rises with the chlorination temperature.

The results of the present research about the Al_4C_3-derived carbon revealed that changes in porosity parameters and the degree of graphitization are in good correlation with specific capacitance values. Capacitance depends on the structure of carbon and varies in the range from 109 to 60 F g^{-1} and from 114 to 64 F g^{-1} for the negatively and positively charged electrode materials, respectively. An exceptionally low capacitance was observed for the material produced at 700 °C. This observation, however, is in good agreement with former studies, which have revealed that at this chlorination temperature aluminum carbide forms a carbon with abnormally low specific surface area due to closed porosity and multiwall nanobarrels, which are formed from the curved graphene flakes [10].

Acknowledgment Dr. Gunnar Svensson (Stockholm University) is acknowledged for the HRTEM pictures.

References

1. Burke AF (2000) J Power Sources 91:37 doi:10.1016/S0378-7753(00)00485-7
2. Leis J, Arulepp M, Lätt M, Kuura H (2005) PCT Patent WO 2005/118471
3. Conway BE (1999) Electrochemical supercapacitors, scientific fundamentals and technological applications. Kluwer Academic/Plenum, New York
4. Largeot C, Portet C, Chmiola J, Taberna PL, Gogotsi Y, Simon P (2008) J Am Chem Soc 130:27 doi:10.1021/ja7106178
5. Gogotsi Y, Nikitin A, Ye H, Zhou W, Fischer JE, Yi B et al (2003) Nat Mater 2:591 doi:10.1038/nmat957
6. Leis J, Arulepp M, Kuura A, Lätt M, Lust E (2006) Carbon 44:2122 doi:10.1016/j.carbon.2006.04.022
7. Arulepp M, Leis J, Lätt M, Miller F, Rumma K, Lust E et al (2006) J Power Sources 162:1460 doi:10.1016/j.jpowsour.2006.08.014
8. Nikitin A, Gogotsi Y (2004) In: Nalwa HS (ed) Encyclopedia of nanoscience and nanotechnology, vol. 7. American Scientific, Stevenson Ranch, pp 553–574
9. Yushin G, Nikitin A, Gogotsi Y (2006) In: Gogotsi Y (ed) Nanomaterials handbook. CRC Press, Taylor & Francis Group, Boca Raton, pp 239–282
10. Leis J, Perkson A, Arulepp M, Käärik M, Svensson G (2001) Carbon 39:2043 doi:10.1016/S0008-6223(01)00020-3
11. Urbonaite S, Juárez-Galán JM, Leis J, Rodríguez-Reinoso F, Svensson G (2008) Microporous Mesoporous Mater 113:1421 doi:10.1016/j.micromeso.2007.10.046
12. Kravchik AE, Osmakov AS, Avarbe RG (1989) Zh Prikladnoy Khim 11:2430, in Russian
13. Leis J, Perkson A, Arulepp M, Nigu P, Svensson G (2002) Carbon 40:1559 doi:10.1016/S0008-6223(02)00019-2
14. Barbieri O, Hahn M, Herzog A, Kötz R (2005) Carbon 43:1303 doi:10.1016/j.carbon.2005.01.001
15. Jänes A, Permann L, Arulepp M, Lust E (2004) Electrochem Commun 6:313 doi:10.1016/j.elecom.2004.01.009
16. Permann L, Lätt M, Leis J, Arulepp M (2006) Electrochim Acta 51:1274 doi:10.1016/j.electacta.2005.06.024
17. Arulepp M, Permann L, Leis J, Perkson A, Rumma K, Jänes A et al (2004) J Power Sources 133:320 doi::10.1016/j.jpowsour.2004.03.026
18. Fernández JA, Arulepp M, Leis J, Stoeckli F, Centeno TA (2008) Electrochim Acta (in press)
19. Lota G, Centeno TA, Frackowiak E, Stoeckli F (2008) Electrochim Acta 53:2210 doi:10.1016/j.electacta.2007.09.028
20. Lust E, Nurk G, Jänes A, Arulepp M, Permann L, Nigu P et al (2002) Condens Matter Phys 5:307